HHS Public Access

Author manuscript

Exp Neurol. Author manuscript; available in PMC 2016 September 30.

White matter injury and microglia/macrophage polarization are strongly linked with age-related long-term deficits in neurological function after stroke

Jun Suenaga[a], **Xiaoming Hu**[a,b,d], **Hongjian Pu**[a,b], **Yejie Shi**[a,d], **Sulaiman Habib Hassan**[a], **Mingyue Xu**[b], **Rehana K. Leak**[c], **R. Anne Stetler**[a,d], **Yanqin Gao**[b], and **Jun Chen**[a,b,d]

[a]Center of Cerebrovascular Disease Research, University of Pittsburgh School of Medicine, Pittsburgh, PA 15213, USA

[b]The State Key Laboratory of Medical Neurobiology, the Institutes of Brain Science and the Collaborative Innovation Center for Brain Science, Fudan University, Shanghai 200032, China

[c]Division of Pharmaceutical Sciences, Duquesne University, Pittsburgh, PA 15282, USA

[d]Geriatric Research, Educational and Clinical Center, Veterans Affairs Pittsburgh Health Care System, Pittsburgh, PA 15261, USA

Abstract

Most of the successes in experimental models of stroke have not translated well to the clinic. One potential reason for this failure is that stroke mainly afflicts the elderly and the majority of experimental stroke studies rely on data gathered from young adult animals. Therefore, in the present study we established a reliable, reproducible model of stroke with low mortality in aged (18 month) male mice and contrasted their pathophysiological changes with those in young (2 month) animals. To this end, mice were subjected to permanent tandem occlusion of the left distal middle cerebral artery (dMCAO) with ipsilateral common carotid artery occlusion (CCAO). Cerebral blood flow (CBF) was evaluated repeatedly during and after stroke. Reduction of CBF was more dramatic and sustained in aged mice. Aged mice exhibited more severe long-term sensorimotor deficits, as manifested by deterioration of performance in the Rotarod and hanging wire tests up to 35d after stroke. Aged mice also exhibited significantly worse long-term cognitive deficits after stroke, as measured by the Morris water maze test. Consistent with these behavioral observations, brain infarct size and neuronal tissue loss after dMCAO were significantly larger in aged mice at 2d and 14d, respectively. The young versus aged difference in neuronal tissue loss, however, did not persist until 35d after dMCAO. In contrast to the transient difference in neuronal tissue loss, we found significant and long lasting deterioration of white matter in aged animals, as revealed by the loss of myelin basic protein (MBP) staining in the striatum at 35d after dMCAO.

*Corresponding author: Dr. Jun Chen, Center of Cerebrovascular Disease Research, University of Pittsburgh School of Medicine, S507 Biomedical Science Tower, 3500 Terrace Street, Pittsburgh, PA 15213, USA, Tel: +1 (412) 648-1263, chenj2@upmc.edu Or Dr. Yanqin Gao, State Key Laboratory of Medical Neurobiology, Fudan University Medical College, Shanghai 200032, China, yqgao@shmu.edu.cn.

We further examined the expression of M1 (CD16/CD32) and M2 (CD206) markers in Iba-1$^+$ microglia by double immunofluorescent staining. In both young and aged mice, the expression of M2 markers peaked around 7d after stroke whereas the expression of M1 markers peaked around 14d after stroke, suggesting a progressive M2-to-M1 phenotype shift in both groups. However, aged mice exhibited significantly reduced M2 polarization compared to young adults. Remarkably, we discovered a strong positive correlation between favorable neurological outcomes after dMCAO and MBP levels or the number of M2 microglia/macrophages. In conclusion, our studies suggest that the distal MCAO stroke model consistently results in ischemic brain injury with long-term behavioral deficits, and is therefore suitable for the evaluation of long-term stroke outcomes. Furthermore, aged mice exhibit deterioration of functional outcomes after stroke and this deterioration is linked to white matter damage and reductions in M2 microglia/macrophage polarization.

Keywords

Aging; microglia; distal middle cerebral artery occlusion (dMCAO); cerebral blood perfusion

Introduction

More than 140,000 people die each year from stroke, the fourth leading cause of death in the United States. Aging is one of the most important risk factors for stroke, as 75% of stroke patients are over the age of 65 according to the Centers for Disease Control and Prevention. Animal models of stroke, particularly in rodents, have provided invaluable *in vivo* experimental platforms to explore therapeutics for stroke and to determine the underlying pathophysiological mechanisms. Although most experimental stroke studies are conducted on healthy young animals, accumulating evidence points to age-related differences in gene expression, cytokine production (Godbout et al., 2005; Kuzumaki et al., 2010; Nolan et al., 2005; Orre et al., 2014; Semple et al., 2013; Ye and Johnson, 2001), microglia/macrophage responses (Hickman et al., 2013; Norden and Godbout, 2013), and white matter vulnerability to ischemia (Rosenzweig and Carmichael, 2013). These age-related changes may explain the current discrepancy between experimental results and clinical outcomes (Ramanantsoa et al., 2013; Tajiri et al., 2013). It is therefore imperative to establish a viable stroke model in aged animals in order to confirm the impact of aging on stroke outcomes and explore the underlying pathophysiology.

Thus far, the small number of studies in aged animals has resulted in controversy regarding short-term outcomes after stroke. Some studies show an age-related increase in infarct volume (Kharlamov et al., 2000; Rosenzweig and Carmichael, 2013; Sutherland et al., 1996), while others reveal significantly smaller infarcts in aged rodents (Liu et al., 2009). This discrepancy may partly be attributed to the use of differing stroke models. In addition, aged animals have seldom been used to study long-term outcomes after stroke due to relatively high mortality. For example, the mortality rate for animals subjected to 60 min proximal middle cerebral artery occlusion (MCAO) is 9% for young adult rats but 43.5% for aged rats (Wang et al., 2003). Similarly, aged rats exposed to 2 hours of proximal MCAO followed by tissue plasminogen activator (tPA) reperfusion suffer from a high mortality rate

(36% at 24h, 50% at 2 d and 60% at 21d) (DiNapoli et al., 2008; Dinapoli et al., 2006; Tan et al., 2013). In contrast to these proximal MCAO models, the distal MCAO model, with permanent coagulation of the MCA distal to the lenticulostriate arteries, causes smaller brain infarcts and does not suffer from high mortality in either young (Kuraoka et al., 2009) or aged rodents (Lubjuhn et al., 2009; Rosell et al., 2013). Thus, the distal MCAO model might be superior to the proximal model for the study of long-term stroke outcomes in aged populations.

In the present study, we found that the distal MCAO model reproducibly results in restricted brain infarcts and long-term neurological deficits with very low mortality rates in aged mice. Thus, this is the first study to explore age-related, long-term differences in brain tissue loss, white matter integrity, and microglia/macrophage responses and to evaluate their potential contribution to sustained functional outcomes after stroke.

Materials and methods

Animals

All animal experiments were approved by the University of Pittsburgh Institutional Animal Care and Use Committee and performed in accordance with the *National Institutes of Health Guide for the Care and Use of Laboratory Animals*. Young male C57BL/6J mice (10-week-old) were obtained from Jackson Laboratory (Bar Harbor, ME, USA) and aged male C57BL/6J mice (18-month-old) were obtained from the National Institute of Aging (NIA) aged mouse colony at Charles River Laboratories (Wilmington, MA, USA). Animals were housed in groups of four per cage in a temperature- and humidity-controlled animal facility with a 12-hour light–dark cycle. Food and water were available *ad libitum*. All efforts were made to minimize animal suffering and the number of animals killed.

Murine model of permanent focal ischemia

All animals were randomly assigned to sham and distal MCAO groups through the use of a lottery-drawing box. Focal cerebral ischemia was produced by permanent distal MCA occlusion, as previously reported (Lubjuhn et al., 2009), plus ipsilateral common carotid artery (CCA) occlusion. Briefly, mice were anesthetized with 1.5% isoflurane in a 30% O2/68.5% N_2O mixture under spontaneous breathing conditions. Rectal temperature was maintained at 37.0°C±0.5°C during surgery with a temperature-regulated heating pad. First, a skin incision was made at the midline of the neck. After being separated from the vagal nerve, the left CCA was exposed and occluded by ligation. The skin was sutured and another skin incision was made between the left eye and the ear. The temporal muscle was dissected by bipolar electrocautery (Bipolar Coagulator, Codman & Shurtleff Inc., Randolph, MA, USA). The temporal muscle temperature was maintained at 37.0°C±0.5°C by a heat lamp. After opening the burr hole and performing a craniotomy, the distal part of the MCA was exposed. The dura mater was then cut and the distal MCA occlusion was completed with low-intensity bipolar electrocautery at the immediate lateral part of the rhinal fissure. Regional cerebral blood flow (CBF) was measured in all stroke animals using laser Doppler flowmetry. Animals that did not show a regional CBF reduction to <30% of pre-ischemia baseline levels were excluded from further experimentation. Sham-operated animals

underwent the same anesthesia and surgical procedures but were not subjected to CCAO and MCAO. All behavioral (sensorimotor and memory tests) and histological (immunostaining and cell counting) assessments were performed by investigators blinded to experimental group assignments. Forty-five young mice and 46 aged mice were used in this study, for a grand total of 91 mice (16 sham-operated and 75 ischemic mice). Only 3 mice died during the perioperative period.

Cortical cerebral blood flow measurements

Real-time 2 dimensional cerebral blood flow was monitored using a laser speckle contrast imager (PeriCam PSI HR System, Perimed, Sweden) as previously described (Lindahl et al., 2013). Select numbers of mice in both groups were subjected to repeated measurements of CBF at 0d (baseline, at left CCAO, and at left distal MCAO), 3d, 7d, 14d, and 21d after dMCAO. After induction of anesthesia, mouse was placed in the prone position, and the skull was exposed through a cut in the skin at the parietal midline. Images were acquired through the laser speckle contrast imager at a working distance of 10 cm from the skull surface. To evaluate CBF changes, the region of interest (ROI) included the left cortical infarct region, which is posterior to the coronal suture and medial to the linear temporalis.

Measurements of infarct volume

For 2,3,5-triphenyltetrazolium chloride (TTC) staining, brains were removed and sliced into 7 coronal sections, each 1 mm thick. Sections were then immersed in prewarmed 2% TTC (Sigma) in saline for 10 min, and then fixed in 4% paraformaldehyde. The neuron-specific marker microtubule associated protein 2 (MAP2) was visualized with anti-MAP2 antibody (Santa Cruz Biotechnology). Infarct volume was determined on these TTC or MAP2-stained sections using NIH Image J software. The actual infarct volume with edema correction was calculated as the volume of the contralateral hemisphere minus the non-infarcted volume of the ipsilateral hemisphere.

Immunohistochemistry and cell counting

Brains were removed following perfusions with saline and 4% paraformaldehyde (Sigma-Aldrich, St Louis, MO, USA) in phosphate-buffered saline (PBS) and then cryoprotected in 30% sucrose in PBS. Following cryoprotection, 25 μm-thick brain sections were cut on a freezing microtome and subjected to immunofluorescence. Primary antibodies include goat anti-CD206 (R&D Systems, Minneapolis, MN, USA), rat anti-CD16/32 (BD, Franklin Lakes, NJ, USA), rabbit anti-myelin basic protein (MBP; Abcam, Cambridge, MA, USA), mouse anti-non-phosphorylated neurofilaments (SMI-32, Abcam), rabbit anti-MAP2 (Santa Cruz Biotechnology, Dallas, TX, USA), and rabbit anti-Iba1 (Wako, Richmond, VA, USA). All images were processed with Image J for counting of automatically recognized cells. Average cell numbers were calculated from 3 randomly selected microscopic fields, and 3 consecutive sections were analyzed for each brain. Data are expressed as mean numbers of cells per square millimeter.

Fluorescence quantification

All fluorescence images were acquired using confocal microscopy (FV1000, Olympus, Tokyo, Japan) and analyzed semi-quantitatively with Image J. For the measurements of MBP staining intensity, the regions of interest (ROI) were set in the striatum. Average staining intensity was calculated from 3 randomly selected microscopic fields in the striatum, and 3 consecutive sections were analyzed for each brain. Data are expressed as the mean intensity of these 9 images from each mouse.

Accelerating Rotarod test

For Rotarod testing, animals were placed on an accelerating rotating rod (4 to 40 rpm over 120s) and their latency to fall off the rod was recorded as previously reported (Bouet et al., 2007). Preoperative training was performed for 3 days with 3 daily trials. The last three trials serve as a preoperative baseline. Postoperative testing was performed at 1, 3, 5, 7, 14, 21, and 35 days after dMCAO, for 3 trials per day, and the mean latency to fall was analyzed.

Hanging wire test

The wire hanging apparatus was comprised of a stainless steel bar (50 cm length; 2 mm diameter), resting on two vertical supports and elevated 37 cm above a flat surface. This test was performed as previously described (Wang et al., 2013). Mice were placed on the bar midway between the supports and were observed for 30 seconds in 4 trials. The amount of time spent hanging was recorded and scored according to the following system: 0, fell off; 1, hung onto the bar with two forepaws; 2, hung onto the bar with added attempt to climb onto the bar; 3, hung onto the bar with two forepaws and one or both hind paws; 4, hung onto the bar with all four paws and with tail wrapped around the bar; 5, escaped to one of the supports.

Morris water maze test

The Morris Water Maze test was carried out as previously described (Bouet et al., 2007; Wang et al., 2013). For this test, an 11-cm square Plexiglas platform was submerged in a circular pool (109 cm diameter) and white, nontoxic tempera paint was added to the water. The platform was submerged 1 cm under the opaque water surface. The water temperature was maintained at 20±1°C and the room temperature was kept at 21±1°C. This test was composed of two parts: the acquisition phase for spatial learning and the memory test. For the acquisition or spatial learning phase, each mouse was released from one of four locations and was allotted 60 seconds to search for the hidden platform 16-20 days after distal MCAO. At the end of each trial, the mouse was placed on the platform or allowed to remain on the platform for 20 seconds with prominent spatial cues displayed around the room. Data from three trials per day for 5 consecutive days were expressed as the time (in seconds) or latency to reach the submerged platform. After the last day of the hidden platform test, a single, 60-second probe trial was performed for the memory test. The platform was removed and each mouse was placed in the pool once for 60 seconds, at the same starting location as was used initially in hidden platform testing. The time spent in the goal quadrant (where the platform had been previously located) and the swim speed were recorded.

Statistical analyses

All data are presented as mean ± standard error of the mean (SEM). Data with two groups were analyzed with the Student's *t*-test (non-directional). For multiple comparisons, the one-way or two-way analysis of variance (ANOVA) was followed by a Tukey *post hoc* test, unless otherwise indicated. The Pearson correlation was also determined. $p<0.05$ was considered statistically significant.

Results

In order to investigate the differences between young and aged mice after stroke injury, we used a tandem occlusion model consisting of left distal middle cerebral artery occlusion (dMCAO) combined with ipsilateral common carotid artery occlusion (CCAO). The overall mortality rate was only 1.3% for young mice (1/79) and 6.5% for aged mice (4/62). These numbers include animals in the current study as well as in preliminary experiments.

Aged mice exhibit greater reductions in cerebral reperfusion after distal MCAO

Cerebral blood flow (CBF) was examined during and after the surgery using 2 dimensional laser speckle imaging. The baseline CBF in the left MCA territories did not show any significant difference between young and aged animals after left CCA ligation (young 358±37 vs aged 328±29, $p>0.05$) (Fig. 1A and 1B). Cerebral perfusion showed a slight decrease but no laterality (Fig. 1B). Immediately after the dMCAO, CBF decreased dramatically on the left side (Fig. 1B, **blue**, Fig. 1C) to less than 1/3 of baseline values. The CBF on the contralateral side was not affected (Fig. 1B, **red**). The CBF in the left MCA territory gradually recovered over time after dMCAO in both young and aged mice, reaching maximal recovery 14d after dMCAO (Fig. 1C, 94.4±33.6 of the baseline in young (blue) and 72.0±7.7% in aged (red), $p>0.05$). However, aged mice showed significantly lower CBF compared to young mice during dMCAO induction (young 35.2±6.6 vs aged 24.3±4.9%, $p<0.05$) and during the course of CBF recovery up to 7d after dMCAO (Fig. 1C). The areas exhibiting less than 30% of baseline CBF (Fig. 1D, **blue**) and between 30-50% of baseline CBF (Fig. 1D, **green**) were also calculated. The area exhibiting less than 30% of baseline CBF was significantly larger in aged mice 14 days after dMCAO, but not at the induction of dMCAO or at 7d post-injury (Fig. 1E). The area exhibiting 30-50% of baseline CBF was also significantly larger in aged mice than in young mice at the induction of dMCAO and at 14d post-injury (Fig. 1F, $p<0.01$, $p<0.05$, respectively). These results suggest that CBF is more compromised in aged animals than in young animals subjected to dMCAO.

Aged mice exhibit greater deterioration in sensorimotor and cognitive functions after dMCAO

Next we evaluated the effect of aging on long-term functional outcomes after dMCAO. The Rotarod tests conducted prior to dMCAO and in sham-operated mice already showed significant age-related differences in the latency to fall (Fig. 2A). This difference may, at least partly, be attributed to the much heavier body weight of aged mice (young 27.6±1.8 vs aged 38.5±3.8g, $p<0.0001$). After dMCAO, there was a transient decline in Rotarod performance in young mice at 1d after dMCAO followed by a rapid recovery (Fig. 2A). In contrast, aged mice exhibited prolonged sensorimotor deficits lasting for at least 35d after

dMCAO (Fig. 2A). Similarly, in the hanging wire test, aged mice exhibited prolonged deficits and delayed recovery after dMCAO compared to young adults (Fig. 2B). These results demonstrate that aging elicits a sustained loss of neurological function after stroke.

Cognitive deficits after dMCAO were assessed by the Morris water maze test. Both young and aged mice experienced difficulty in locating the hidden platform after dMCAO (Fig. 2C and 2D), suggesting impaired cognition in both groups. Similarly, both young and aged groups spent much shorter time in the target quadrant when the platform was removed, suggesting impaired memory after dMCAO (Fig. 2C and 2E). As expected, aged dMCAO mice demonstrated significantly worse cognitive (Fig. 2D) and memory (Fig. 2E) deficits compared to young adults. There was no difference in swim speed between any groups (Fig. 2F).

Distal MCAO results in enlarged brain infarcts in aged mice

Consistent with previous reports (Carmichael, 2005), dMCAO resulted in a cerebral infarct that was mainly restricted to the cortex, the underlying white matter, and a small portion of striatum. Within the cerebral cortex, the infarct area corresponded with the MCA perfusion territory whereas there was preservation of the anterior cerebral artery (ACA) and posterior cerebral artery (PCA) regions (Fig. 3A). Hippocampal, thalamic, and occipital areas (PCA distribution) and the brainstem [vertebrobasilar artery (VA) distribution] all remained intact, as confirmed by TTC staining. Compared to young adults, aged mice exhibited significantly larger infarct areas in the cortex (young 15.5±1.0 *vs* aged 18.7±0.9%, $p<0.05$) and striatum (young 0.1±0.1 vs aged 2.0±0.7%, $p<0.05$), resulting in enlarged total area of infarct in the ischemic hemisphere (young 15.6±1.1 vs aged 20.7±0.9%, $p<0.01$) at 2d after dMCAO (Fig. 3B-3D). The enlarged infarct region in the striatum in aged mice was mainly localized to the dorsolateral quadrant, which corresponds roughly to the putamen in humans (Fig. 3A, **dotted area**). Although aged mice exhibited increased neuronal tissue loss at 14d after dMCAO, this difference disappeared by 35d post injury, as measured by the area of MAP2 loss (Fig.3E). There was no significant difference in brain size between young and aged mice (young 124.5±8.1 mm^3, aged 118.1±3.0 mm^3, $p>0.05$). These histological data, considered together with the long-term behavioral deficits in aged mice, support the involvement of non-neuronal mechanism(s) in sustained age-related neurological deficits after dMCAO.

White matter injury may contribute to age-related functional deficits at late stages after dMCAO

The severity of white matter injury is an important contributing factor for long-term motor and cognitive decline after stroke (Kissela et al., 2009). Therefore, we examined white matter integrity, including myelin integrity and axonal damage, by immunostaining for myelin basic protein (MBP) and non-phosphorylated pathological neurofilaments (SMI-32), respectively. Interestingly, young and aged brains from sham animals demonstrated marked differences in white matter structures in the white matter-enriched striatum (Fig. 4A-4B), as manifested by age-related reductions in MBP intensity (indicating loss of myelin integrity) and increased SMI-32 staining (indicating axonal demyelination). SMI32 is a marker of non-phosphorylated neurofilaments. Neurofilaments are important components of axon, and thus

increased SMI32 indicates increased axonal damage. Loss of white matter integrity was also observed in the uninjured cortex in aged mice (data not shown). Quantification of MBP staining after sham operation or dMCAO demonstrated the same trends in both young and aged mice, with an early increase in MBP expression 1d after dMCAO followed by a gradual decrease in MBP intensity until at least 35d after injury (Fig. 4C). At all the time points tested, there were significant higher levels of MBP in young mice than in aged mice (Fig. 4C). The intensity of MBP staining exhibited a positive correlation with sensorimotor performance at 35d after dMCAO (Fig. 4D, r=0.5843, $p<0.0001$) and with memory function at 21d after dMCAO (Fig 4E, r=0.7017, $p<0.0001$) in young and aged mice. These results indicate that the dramatic loss of white matter integrity might be an important factor dictating long-term behavioral deficits in aged mice. There was an inverse correlation between MBP and SMI-32 staining intensity in the striatum of aged mice (Fig 4F, r= −0.6123, $p=0.0005$), suggesting a close relationship between demyelination and axonal damage after dMCAO. This correlation, however, was not apparent in young animals (Fig 4G), suggesting that the viability of the myelin sheath may not be accompanied by superior axonal health in young mice after dMCAO.

Reductions in M2 microglia/macrophages are linked to age-related deterioration in neurological function at late stages of dMCAO

Microglia/macrophages respond dynamically to ischemic injury by assuming diverse phenotypes. Our previous studies using the transient MCAO model in young mice documented a shift of microglia/macrophages from the protective M2 phenotype to the toxic M1 phenotype (Hu et al., 2012). Here, we found a similar trend in microglia/macrophage polarization after dMCAO in both young and aged mice. Double immunofluorescence staining of CD206, an M2 marker, and the microglia/macrophage marker Iba-1 revealed a peak in the M2 phenotype 7d after dMCAO (Fig. 6A-6B). In contrast, the M1 polarization marker CD16/32 demonstrated a delayed peak at 14d after dMCAO (Fig. 5B-5C). Notably, aged animals exhibited a dramatic elevation in the number of $CD16/32^{+}Iba\text{-}1^{+}$ M1 microglia/macrophages under sham conditions. This M1 shift was maintained in aged mice until 3d after dMCAO (Fig. 5C). In addition, the number of M2 microglia/macrophages was significantly lower in aged mice after dMCAO (Fig 6B). Taken together, these data suggest that microglia/macrophages are primed toward the M1 phenotype in aged mice even in the absence of an ischemic challenge. After ischemic injury, the aged brain assumed M1 polarization soon after dMCAO and demonstrated a long-lasting impairment in M2 responses. A strong positive correlation between the number of M2 cells and behavioral performance on the Rotarod was apparent at late stages after dMCAO (Fig. 6C). Similarly, there was a positive correlation between M2 expression and performance in the Water maze test. Finally, we discovered a positive correlation between the number of M2 cells and MBP intensity in the striatum at 35d after dMCAO (Fig. 6E), supporting the hypothesis that M2 microglial/macrophage polarization is linked with the degree of myelination long after stroke onset. These results suggest that impaired M2 responses in aged mice might be an important factor determining long-term functional deficits and white matter integrity.

Discussion

The goals of the present study were to contrast the responses of young and aged animals to stroke injury and begin to elucidate the mechanism(s) underlying poor stroke outcomes in the aged population. First we established a robust, reproducible model of age-related deficits after stroke injury. Using a permanent distal MCAO model with CCAO, we were able to measure long-term sensorimotor deficits in aged animals. Unlike in aged animals, sensorimotor functions in young adults underwent early, transient deficits after stroke and recovered quickly. Memory function was already impaired in aged sham animals compared to young controls. These baseline spatial memory deficits are consistent with previous reports in aging rodents (Bach et al., 1999) and elderly humans (Gazova et al., 2013). Spatial learning abilities in aged sham mice were decreased but not statistically significant as compared to young shams. Age-related deficits in spatial learning have been observed in previous studies (Krause et al., 2008; Murchison et al., 2009); thus, the absence of significant age-related deficits in spatial learning in the present study might due to procedural differences from previous reports. Cognitive function after dMCAO was impaired in both young and aged groups, but the aged mice exhibited significantly worse learning and memory deficits than young mice. The mortality rate of this model in aged mice (6.5%) is much lower relative to other intraluminal MCAO models (Wang et al., 2003). Therefore, the dMCAO model is a valuable tool to evaluate long-term stroke outcomes in aged animals.

Although the MCA was permanently occluded in our distal MCAO model, cerebral perfusion gradually recovered after stroke in the ischemic region. Our CBF data reveal a slower rate of CBF recovery after dMCAO in aged mice. The ischemic penumbra is defined as the region where CBF decreases to 30-50% of baseline (Mayer et al., 2000). As expected, this area was much larger in aged mice. Previous studies have shown that mild cerebral hypoperfusion can disrupt axonal and glial integrity in white matter tracts (Reimer et al., 2011). After prolonged cerebral hypoperfusion, oxidative stress also interferes with white matter repair by disrupting oligodendrocyte precursor cell renewal (Miyamoto et al., 2013). Therefore, prolonged hypoperfusion in aged brains after stroke likely leads to damage in both grey and white matter.

In agreement with our CBF data, we found that the aged mice subjected to dMCAO exhibited significantly larger infarct regions in both the cortex and striatum. This finding is also consistent with previous studies showing larger infarct volumes and less functional recovery in aged mice (DiNapoli et al., 2008; Dinapoli et al., 2006; Dong et al., 2014; Rosen et al., 2005; Tan et al., 2009). We found that the striatum was especially affected in the aged animals after stroke. Previous studies using permanent distal MCAO without CCAO for young mice reported that the infarct region was restricted to the cortex (Guo et al., 2009; Kuraoka et al., 2009; Lubjuhn et al., 2009). The striatum is supplied by the lenticulostriate arteries (LSA), which originates from the proximal MCA (Yamori et al., 1976), and is usually spared in the dMCAO model in young adults. The greater involvement of this area in aged mice might reflect additional occlusion of the CCA, lower arterial blood pressure during ischemia (Rosen et al., 2005), and lower CBF during and after ischemia in aged animals.

The present study demonstrates that aged animals exhibit deterioration in long-term neurological deficits lasting until 35d after dMCAO. By this timepoint, the CBF and neuronal tissue loss in aged animals are no different from young adults. This result prompts us to speculate that other non-neuronal mechanism(s) contribute to long lasting functional deficits in aged mice at late stages of stroke. Our studies demonstrate that prolonged white matter injury and unfavorable microglia/macrophage responses are linked to long-term neurological deficits. Aged mice are known to be more sensitive than young adults to white matter stroke, as manifested by increased oligodendrocyte cell death, elevated oxidative damage, and greater secondary white matter atrophy (Rosenzweig and Carmichael, 2013). Consistent with these observations, our studies show that aged mice exhibit greater white matter damage in the striatum in the late stages after stroke, in addition to increased striatal infarct volume in early stages. The striatum receives dense projections from the cerebral cortex and sends efferent projections to the other parts of the basal ganglia (Gerfen et al., 2002). Furthermore, the striatum is well known to be important in the planning and modulation of movements and in cognitive processes such as working memory (Voytek and Knight, 2010). Thus, deterioration of white matter in the striatum of aged mice may be an important contributor to long-lasting functional deficits in old mice and represents a therapeutic target for elderly stroke victims.

Aside from white matter injury, a second factor found to be correlated with age-related exacerbation of functional deficits was microglia/macrophage phenotype. Microglia/macrophage are potent modulators of CNS repair and regeneration (Hu et al., 2015; Savman et al., 2013). These highly plastic cells assume diverse phenotypes and play dualistic roles in brain injury and recovery. Classically activated M1 microglia/macrophages are pro-inflammatory and exert detrimental effects on the ischemic brain, whereas alternatively activated M2 microglia/macrophages are anti-inflammatory and protective (Hu et al., 2014; Seifert and Pennypacker, 2014). Both young and aged dMCAO groups exhibited a similar M2-to-M1 switch as previously reported using the proximal MCAO model (Hu et al., 2012). Furthermore, we found that aged mice exhibited a reduced M2 polarization and increased M1 polarization compared to young adults. These findings are consistent with accumulating evidence showing age-related shifts in microglia towards a pro-inflammatory state (Dilger and Johnson, 2008; Norden and Godbout, 2013). For example, microarray studies indicate that aged brains exhibit increases in the levels of inflammatory and pro-oxidant genes and decreases in the levels of growth factor genes and anti-oxidant genes (Godbout et al., 2005; Orre et al., 2014). In addition, there are increased levels of pro-inflammatory cytokines (Godbout et al., 2005; Kuzumaki et al., 2010) and decreased levels of anti-inflammatory cytokines in the aged brain (Nolan et al., 2005; Ye and Johnson, 2001). Our study indicates that reductions in M2 polarization, but not increases in M1 polarization, are correlated with exaggerated behavioral deficits and white matter injury at late stages of stroke. These findings might reflect the importance of M2 microglia/macrophages in brain repair (Hu et al., 2015). M2 microglia/macrophages appear to promote multiple brain repair responses, such as neurogenesis, angiogenesis, and white matter repair by resolving local inflammation and releasing trophic factors (An et al., 2014; Hu et al., 2015; Wang et al., 2015). Consistent with these functional roles, M2 microglial/macrophage phenotype was correlated with

myelin integrity in the present study. Thus, promoting microglia/macrophage M2 phenotypic changes might also help promote stroke recovery in elderly stroke victims.

In conclusion, aged mice exhibited greater deterioration in functional outcomes than young mice, and these effects were associated with reduced cerebral perfusion, larger infarct volumes, white matter injury, and dysregulation of M2 microglia/macrophage polarization. White matter injury and impaired M2 polarization were strongly correlated with long-term functional deficits and might serve as future therapeutic targets to promote post-stroke recovery.

Acknowledgments

This work was supported by U.S. National Institutes of Health grants NS36736, NS43802, NS45048 and NS089534 (to JC), U.S. Department of Veterans Affairs Research Career Scientist Award and RR&D Merit Review (to JC), the Rotary Foundation Global Scholarship Grants GG1412044 (to JS), American Heart Association Scientist Development Grant 13SDG14570025 (to XH) and Postdoctoral Fellowship Award 15POST22260011 (to YS), and Chinese Natural Science Foundation grants 81020108021, 81171149, 81371306 and J1210041 (to YG), and 81228008 (to JC).

References

An C, Shi Y, Li P, Hu X, Gan Y, Stetler RA, Leak RK, Gao Y, Sun BL, Zheng P, Chen J. Molecular dialogs between the ischemic brain and the peripheral immune system: dualistic roles in injury and repair. Prog Neurobiol. 2014; 115:6–24. [PubMed: 24374228]

Bach ME, Barad M, Son H, Zhuo M, Lu YF, Shih R, Mansuy I, Hawkins RD, Kandel ER. Age-related defects in spatial memory are correlated with defects in the late phase of hippocampal long-term potentiation in vitro and are attenuated by drugs that enhance the cAMP signaling pathway. Proc Natl Acad Sci USA. 1999; 96:5280–5285. [PubMed: 10220457]

Bouet V, Freret T, Toutain J, Divoux D, Boulouard M, Schumann-Bard P. Sensorimotor and cognitive deficits after transient middle cerebral artery occlusion in the mouse. Exp Neurol. 2007; 203:555–567. [PubMed: 17067578]

Carmichael ST. Rodent models of focal stroke: size, mechanism, and purpose. NeuroRx. 2005; 2:396–409. [PubMed: 16389304]

Dilger RN, Johnson RW. Aging, microglial cell priming, and the discordant central inflammatory response to signals from the peripheral immune system. J Leukoc Biol. 2008; 84:932–939. [PubMed: 18495785]

DiNapoli VA, Huber JD, Houser K, Li X, Rosen CL. Early disruptions of the blood-brain barrier may contribute to exacerbated neuronal damage and prolonged functional recovery following stroke in aged rats. Neurobiol Aging. 2008; 29:753–764. [PubMed: 17241702]

Dinapoli VA, Rosen CL, Nagamine T, Crocco T. Selective MCA occlusion: a precise embolic stroke model. J Neurosci Methods. 2006; 154:233–238. [PubMed: 16472870]

Dong P, Zhao J, Zhang Y, Dong J, Zhang L, Li D, Li L, Zhang X, Yang B, Lei W. Aging causes exacerbated ischemic brain injury and failure of sevoflurane post-conditioning: role of B-cell lymphoma-2. Neuroscience. 2014; 275:2–11. [PubMed: 24929064]

Gazova I, Laczo J, Rubinova E, Mokrisova I, Hyncicova E, Andel R, Vyhnalek M, Sheardova K, Coulson EJ, Hort J. Spatial navigation in young versus older adults. Front Aging Neurosci. 2013; 5:94. [PubMed: 24391585]

Gerfen CR, Miyachi S, Paletzki R, Brown P. D1 dopamine receptor supersensitivity in the dopamine-depleted striatum results from a switch in the regulation of ERK1/2/MAP kinase. J Neurosci. 2002; 22:5042–5054. [PubMed: 12077200]

Godbout JP, Chen J, Abraham J, Richwine AF, Berg BM, Kelley KW, Johnson RW. Exaggerated neuroinflammation and sickness behavior in aged mice following activation of the peripheral innate immune system. Faseb j. 2005; 19:1329–1331. [PubMed: 15919760]

Guo Q, Wang G, Liu X, Namura S. Effects of gemfibrozil on outcome after permanent middle cerebral artery occlusion in mice. Brain Res. 2009; 1279:121–130. [PubMed: 19427843]

Hickman SE, Kingery ND, Ohsumi TK, Borowsky ML, Wang LC, Means TK, El Khoury J. The microglial sensome revealed by direct RNA sequencing. Nat Neurosci. 2013; 16:1896–1905. [PubMed: 24162652]

Hu X, Leak RK, Shi Y, Suenaga J, Gao Y, Zheng P, Chen J. Microglial and macrophage polarization-new prospects for brain repair. Nat Rev Neurol. 2015; 11:56–64. [PubMed: 25385337]

Hu X, Li P, Guo Y, Wang H, Leak RK, Chen S, Gao Y, Chen J. Microglia/macrophage polarization dynamics reveal novel mechanism of injury expansion after focal cerebral ischemia. Stroke. 2012; 43:3063–3070. [PubMed: 22933588]

Hu X, Liou AK, Leak RK, Xu M, An C, Suenaga J, Shi Y, Gao Y, Zheng P, Chen J. Neurobiology of microglial action in CNS injuries: receptor-mediated signaling mechanisms and functional roles. Prog Neurobiol. 2014; 119-120:60–84. [PubMed: 24923657]

Kharlamov A, Kharlamov E, Armstrong DM. Age-dependent increase in infarct volume following photochemically induced cerebral infarction: putative role of astroglia. J Gerontol A Biol Sci Med Sci. 2000; 55:B135–141. discussion B142-133. [PubMed: 10795717]

Kissela B, Lindsell CJ, Kleindorfer D, Alwell K, Moomaw CJ, Woo D, Flaherty ML, Air E, Broderick J, Tsevat J. Clinical prediction of functional outcome after ischemic stroke: the surprising importance of periventricular white matter disease and race. Stroke. 2009; 40:530–536. [PubMed: 19109548]

Krause M, Yang Z, Rao G, Houston FP, Barnes CA. Altered dendritic integration in hippocampal granule cells of spatial learning-impaired aged rats. J Neurophysiol. 2008; 99:2769–2778. [PubMed: 18417628]

Kuraoka M, Furuta T, Matsuwaki T, Omatsu T, Ishii Y, Kyuwa S, Yoshikawa Y. Direct experimental occlusion of the distal middle cerebral artery induces high reproducibility of brain ischemia in mice. Exp Anim. 2009; 58:19–29. [PubMed: 19151508]

Kuzumaki N, Ikegami D, Imai S, Narita M, Tamura R, Yajima M, Suzuki A, Miyashita K, Niikura K, Takeshima H, Ando T, Ushijima T, Suzuki T, Narita M. Enhanced IL-1beta production in response to the activation of hippocampal glial cells impairs neurogenesis in aged mice. Synapse. 2010; 64:721–728. [PubMed: 20336624]

Lindahl F, Tesselaar E, Sjoberg F. Assessing paediatric scald injuries using Laser Speckle Contrast Imaging. Burns. 2013; 39:662–666. [PubMed: 23092702]

Liu F, Yuan R, Benashski SE, McCullough LD. Changes in experimental stroke outcome across the life span. J Cereb Blood Flow Metab. 2009; 29:792–802. [PubMed: 19223913]

Lubjuhn J, Gastens A, von Wilpert G, Bargiotas P, Herrmann O, Murikinati S, Rabie T, Marti HH, Amende I, Hampton TG, Schwaninger M. Functional testing in a mouse stroke model induced by occlusion of the distal middle cerebral artery. J Neurosci Methods. 2009; 184:95–103. [PubMed: 19660497]

Mayer TE, Hamann GF, Baranczyk J, Rosengarten B, Klotz E, Wiesmann M, Missler U, Schulte-Altedorneburg G, Brueckmann HJ. Dynamic CT perfusion imaging of acute stroke. AJNR Am J Neuroradiol. 2000; 21:1441–1449. [PubMed: 11003276]

Miyamoto N, Maki T, Pham LD, Hayakawa K, Seo JH, Mandeville ET, Mandeville JB, Kim KW, Lo EH, Arai K. Oxidative stress interferes with white matter renewal after prolonged cerebral hypoperfusion in mice. Stroke. 2013; 44:3516–3521. [PubMed: 24072001]

Murchison D, McDermott AN, Lasarge CL, Peebles KA, Bizon JL, Griffith WH. Enhanced calcium buffering in F344 rat cholinergic basal forebrain neurons is associated with age-related cognitive impairment. J Neurophysiol. 2009; 102:2194–2207. [PubMed: 19675291]

Nolan Y, Maher FO, Martin DS, Clarke RM, Brady MT, Bolton AE, Mills KH, Lynch MA. Role of interleukin-4 in regulation of age-related inflammatory changes in the hippocampus. J Biol Chem. 2005; 280:9354–9362. [PubMed: 15615726]

Norden DM, Godbout JP. Review: microglia of the aged brain: primed to be activated and resistant to regulation. Neuropathol Appl Neurobiol. 2013; 39:19–34. [PubMed: 23039106]

Orre M, Kamphuis W, Osborn LM, Melief J, Kooijman L, Huitinga I, Klooster J, Bossers K, Hol EM. Acute isolation and transcriptome characterization of cortical astrocytes and microglia from young and aged mice. Neurobiol Aging. 2014; 35:1–14. [PubMed: 23954174]

Ramanantsoa N, Fleiss B, Bouslama M, Matrot B, Schwendimann L, Cohen-Salmon C, Gressens P, Gallego J. Bench to cribside: the path for developing a neuroprotectant. Transl Stroke Res. 2013; 4:258–277. [PubMed: 24323277]

Reimer MM, McQueen J, Searcy L, Scullion G, Zonta B, Desmazieres A, Holland PR, Smith J, Gliddon C, Wood ER, Herzyk P, Brophy PJ, McCulloch J, Horsburgh K. Rapid disruption of axon-glial integrity in response to mild cerebral hypoperfusion. J Neurosci. 2011; 31:18185–18194. [PubMed: 22159130]

Rosell A, Agin V, Rahman M, Morancho A, Ali C, Koistinaho J, Wang X, Vivien D, Schwaninger M, Montaner J. Distal occlusion of the middle cerebral artery in mice: are we ready to assess long-term functional outcome? Transl Stroke Res. 2013; 4:297–307. [PubMed: 24323300]

Rosen CL, Dinapoli VA, Nagamine T, Crocco T. Influence of age on stroke outcome following transient focal ischemia. J Neurosurg. 2005; 103:687–694. [PubMed: 16266051]

Rosenzweig S, Carmichael ST. Age-dependent exacerbation of white matter stroke outcomes: a role for oxidative damage and inflammatory mediators. Stroke. 2013; 44:2579–2586. [PubMed: 23868277]

Savman K, Heyes MP, Svedin P, Karlsson A. Microglia/macrophage-derived inflammatory mediators galectin-3 and quinolinic acid are elevated in cerebrospinal fluid from newborn infants after birth asphyxia. Transl Stroke Res. 2013; 4:228–235. [PubMed: 23807898]

Seifert HA, Pennypacker KR. Molecular and cellular immune responses to ischemic brain injury. Transl Stroke Res. 2014; 5:543–553. [PubMed: 24895236]

Semple BD, Blomgren K, Gimlin K, Ferriero DM, Noble-Haeusslein LJ. Brain development in rodents and humans: Identifying benchmarks of maturation and vulnerability to injury across species. Prog Neurobiol. 2013; 106-107:1–16. [PubMed: 23583307]

Sutherland GR, Dix GA, Auer RN. Effect of age in rodent models of focal and forebrain ischemia. Stroke. 1996; 27:1663–1667. discussion 1668. [PubMed: 8784145]

Tajiri N, Dailey T, Metcalf C, Mosley YI, Lau T, Staples M, van Loveren H, Kim SU, Yamashima T, Yasuhara T, Date I, Kaneko Y, Borlongan CV. In vivo animal stroke models: a rationale for rodent and non-human primate models. Transl Stroke Res. 2013; 4:308–321. [PubMed: 23682299]

Tan Z, Li X, Kelly KA, Rosen CL, Huber JD. Plasminogen activator inhibitor type 1 derived peptide, EEIIMD, diminishes cortical infarct but fails to improve neurological function in aged rats following middle cerebral artery occlusion. Brain Res. 2009; 1281:84–90. [PubMed: 19465008]

Tan Z, Turner RC, Leon RL, Li X, Hongpaisan J, Zheng W, Logsdon AF, Naser ZJ, Alkon DL, Rosen CL, Huber JD. Bryostatin improves survival and reduces ischemic brain injury in aged rats after acute ischemic stroke. Stroke. 2013; 44:3490–3497. [PubMed: 24172582]

Voytek B, Knight RT. Prefrontal cortex and basal ganglia contributions to visual working memory. Proc Natl Acad Sci USA. 2010; 107:18167–18172. [PubMed: 20921401]

Wang G, Jiang X, Pu H, Zhang W, An C, Hu X, Liou AK, Leak RK, Gao Y, Chen J. Scriptaid, a novel histone deacetylase inhibitor, protects against traumatic brain injury via modulation of PTEN and AKT pathway: scriptaid protects against TBI via AKT. Neurotherapeutics. 2013; 10:124–142. [PubMed: 23132328]

Wang G, Shi Y, Jiang X, Leak RK, Hu X, Wu Y, Pu H, Li WW, Tang B, Wang Y, Gao Y, Zheng P, Bennett MV, Chen J. HDAC inhibition prevents white matter injury by modulating microglia/macrophage polarization through the GSK3beta/PTEN/Akt axis. Proc Natl Acad Sci USA. 2015; 112:2853–2858. [PubMed: 25691750]

Wang RY, Wang PS, Yang YR. Effect of age in rats following middle cerebral artery occlusion. Gerontology. 2003; 49:27–32. [PubMed: 12457047]

Yamori Y, Horie R, Handa H, Sato M, Fukase M. Pathogenetic similarity of strokes in stroke-prone spontaneously hypertensive rats and humans. Stroke. 1976; 7:46–53. [PubMed: 1258104]

Ye SM, Johnson RW. An age-related decline in interleukin-10 may contribute to the increased expression of interleukin-6 in brain of aged mice. Neuroimmunomodulation. 2001; 9:183–192. [PubMed: 11847480]

Highlights

- The distal MCAO model is suitable for the evaluation of long-term stroke outcomes
- Aged mice exhibit more deterioration in functional outcomes after distal MCAO
- White matter injury correlates with long-term functional deficits after dMCAO
- Loss of M2 microglia/macrophages correlates with long-term functional deficits

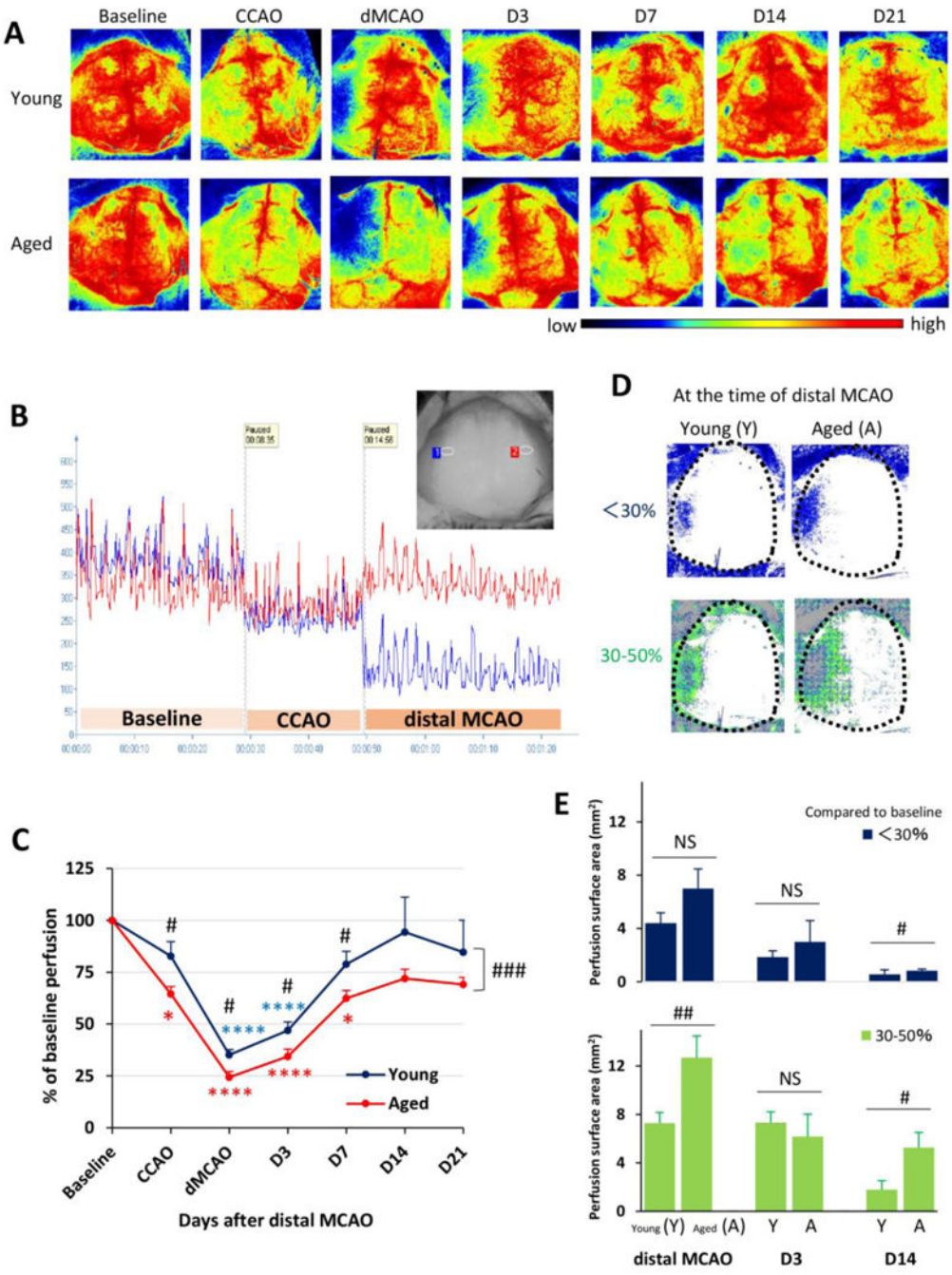

Fig. 1. Aged mice exhibit reduced cerebral reperfusion over time after distal MCAO

Cerebral blood flow (CBF) was monitored using the 2 dimensional laser speckle technique at 0d (baseline, after CCAO, and after distal MCAO), 3d, 7d, 14d, and 21d after distal MCAO. **A.** Representative 2-D laser speckle images in young and aged groups. Images represent the axial surface view from the top. The left side of the picture designates the left infarct region. **B.** Representative recordings of CBF in young animals before and 0d after dMCAO. The inset shows two recording areas in the infarct region (blue) and the counterpart on the contralateral side (red). **C.** CBF in the infarct region was quantified and

expressed as percent change from baseline (pre-dMCAO). Data are means ± SEM. n=4 per group. *$p \leq 0.05$, ****$p \leq 0.0001$ vs corresponding baseline. $^{\#}p \leq 0.05$, $^{\#\#\#}p \leq 0.001$, young vs aged. **D.** Representative images of surface areas where the CBF decreased to less than 30% (blue), or between 30-50% (green) of baseline at 0d after dMCAO. **E.** Quantification of surface areas where the CBF decreased to less than 30% (blue), or between 30-50% (green) of baseline at 0d, 3d and 14d after dMCAO. Data are means ± SEM. n=4 per group. $^{\#}p \leq 0.05$; $^{\#\#}p \leq 0.01$; NS, not significant.

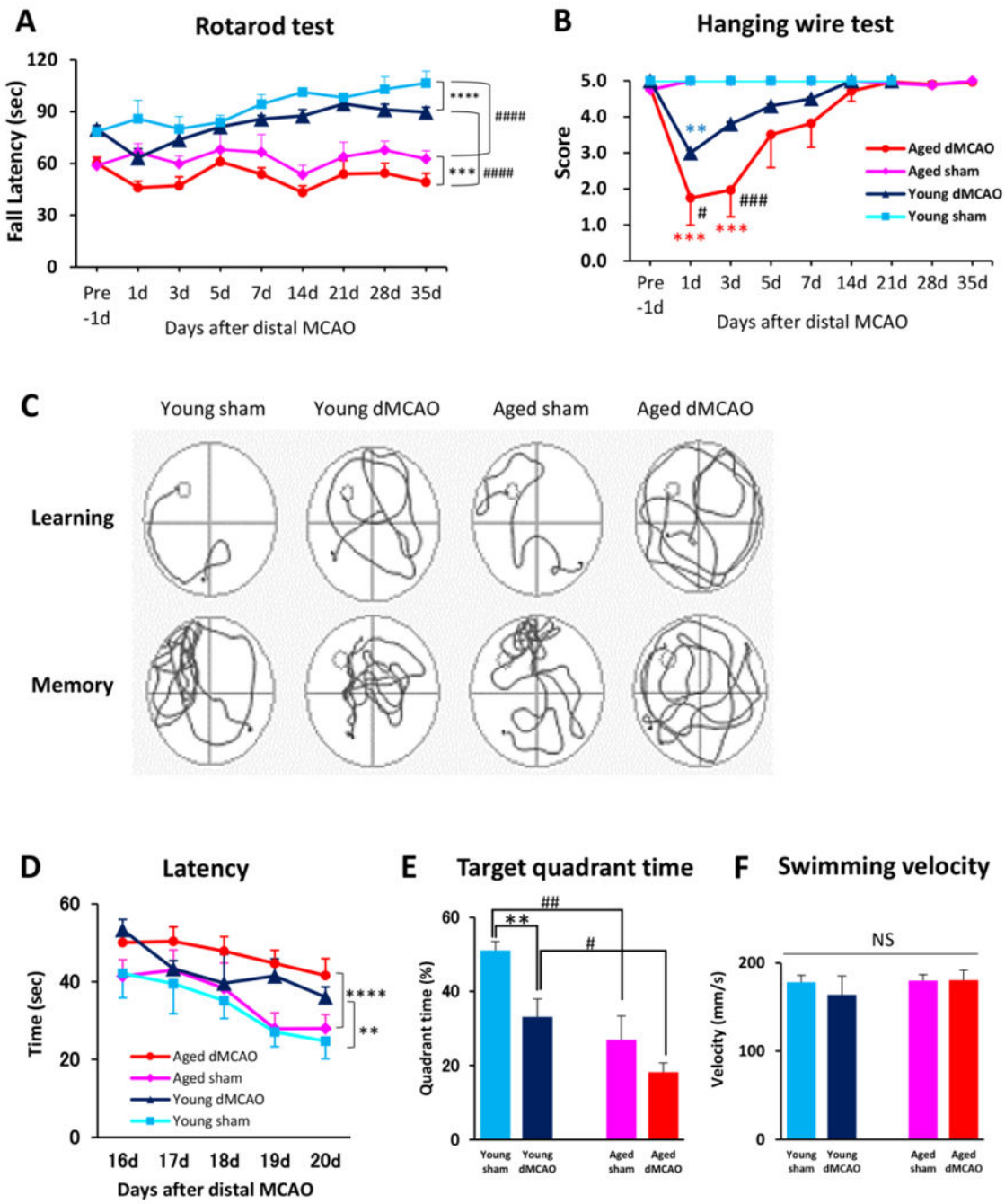

Fig. 2. Aged mice show greater deterioration in sensorimotor and cognitive functions after dMCAO

A-B. Sensorimotor functions were evaluated up to 35d after dMCAO or sham operation in young and aged mice. n=8/group. Shown are the mean ± SEM. **A.** Rotarod test. *** $p \leq 0.001$, **** $p \leq 0.0001$, #### $p \leq 0.0001$. **B.** Hanging wire test. ** $p \leq 0.01$, *** $p \leq 0.001$ vs corresponding sham, # $p \leq 0.05$, ### $p \leq 0.001$ vs. young dMCAO. **C-F.** Long-term cognitive functions were assessed by the Morris water maze. n=8/group. Shown are the mean ± SEM. **C.** Representative images of the swim paths of mice in each group while the platform was

present (learning phase) and after it was removed (memory phase). **D.** More severe learning deficits were observed in aged mice, as reflected by longer escape time. ** $p \leq 0.01$, **** $p \leq 0.0001$ vs corresponding sham. **E.** More severe memory deficits were observed in aged mice, as reflected by shorter time spent in the target quadrant. ** $p \leq 0.01$, $^{\#}$ $p \leq 0.05$, $^{\#\#}$ $p \leq 0.01$. **F.** Both groups had similar swim speeds, thereby showing equivalent motor skills. ns: no significance.

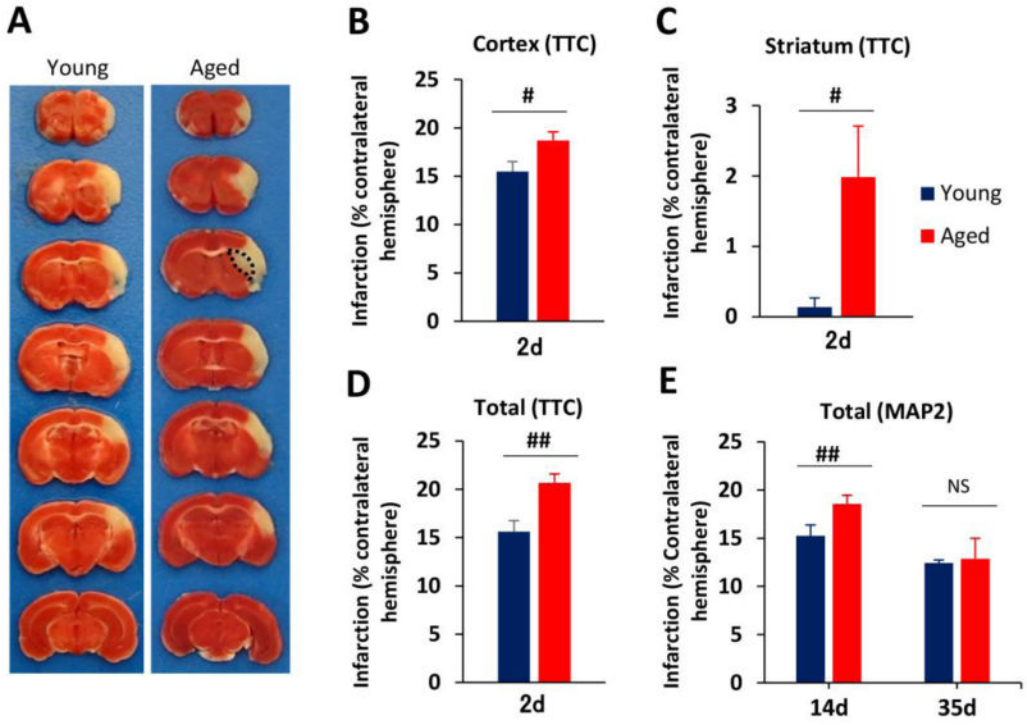

Fig. 3. Distal MCAO results in larger brain infarct volumes soon after stroke in aged mice compared to young adult mice

A. Representative TTC staining at 2d after distal MCAO in young and aged mice. Black dotted line in brain sections from aged mice designates the additional infarct area in the striatum. **B-D.** Quantification of infarct volume at 2d after dMCAO in young and aged mice. Infarct sizes were expressed as percentages of the contralateral hemisphere in the cortex (**B**), striatum (**C**) and total hemisphere (**D**). Values are means ± SEM. n=4 per group. $^{\#}p \leq 0.05$, $^{\#\#}p \leq 0.01$. **B-D**, Quantification of brain tissue loss at 14d and 35d after dMCAO in young and aged mice, as determined by immunostaining for the neuronal marker MAP2. Values are means ± SEM. n=4 per group. $^{\#\#}p \leq 0.01$; ns: no significance.

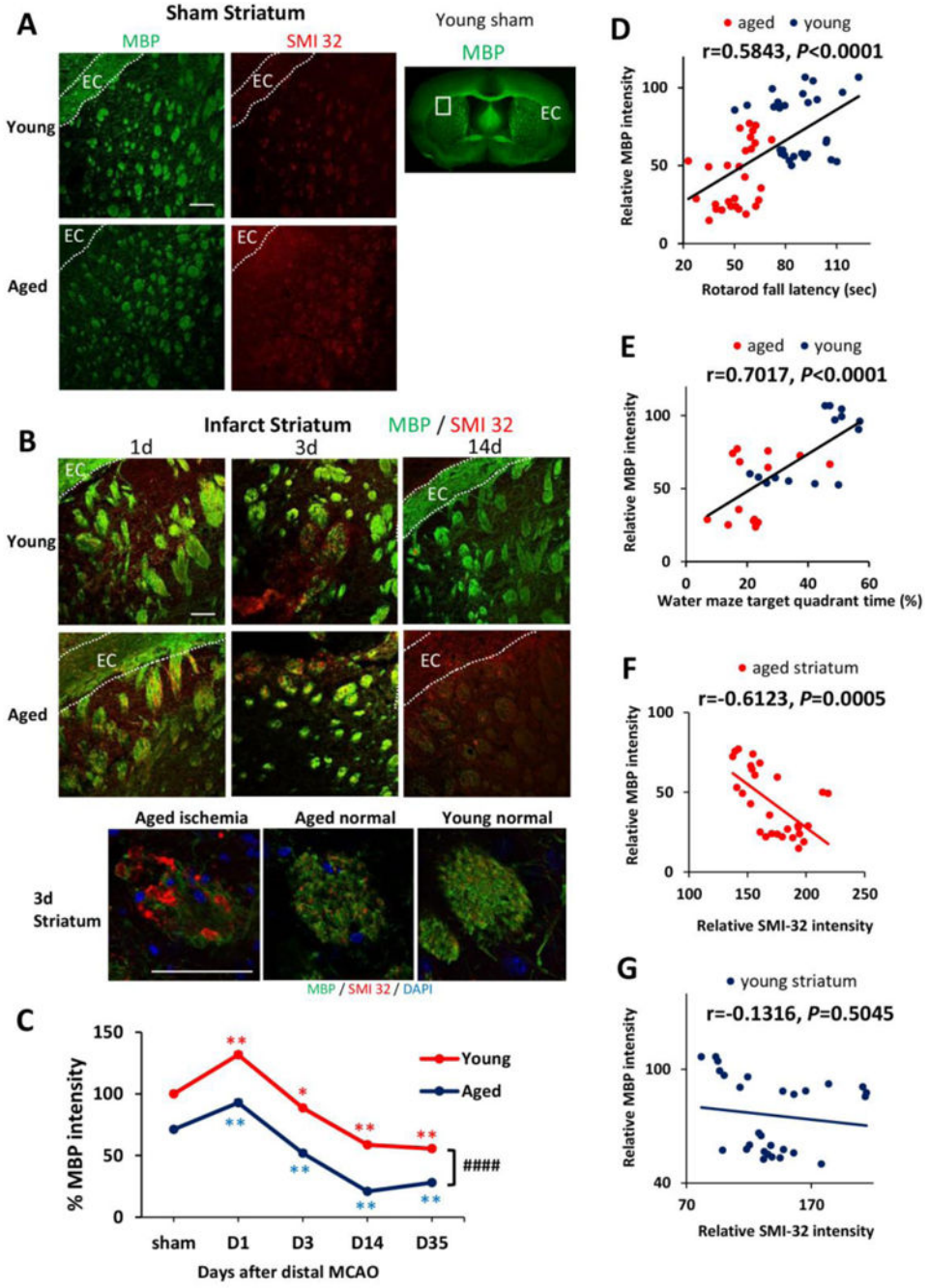

Fig. 4. White matter injury in aged mice is linked with functional deficits at late stages of dMCAO

A. MBP and SMI-32 staining in sham-operated young and aged mice. White squares in lower magnification views of MBP staining designate the area shown under high magnification on the left. EC, external capsule. **B.** Representative images of MBP and SMI-32 double-staining at 1, 3, and 14d after dMCAO in young and aged mice. Scale bar: 100 μm. High power images of the striatum at 3d after dMCAO were shown in lower panels. Scale bar: 50 μm. **C.** Quantification of MBP staining intensities in the striatum in young and

aged mice after sham-operation or at 1, 3, 14, and 35 days after dMCAO. Data were expressed as percentage of young sham. n=7 per group. *$p \leq 0.05$, **$p \leq 0.01$, vs corresponding sham. $^{\#\#\#\#}p \leq 0.0001$ young vs aged. **D-E.** Pearson correlation between MBP staining intensity and behavioral performance on the Rotarod or Morris water maze memory tests. **D.** There was a positive correlation between MBP staining intensity and Rotarod performance at 35d after dMCAO. **E.** There was a positive correlation between MBP intensity and water maze performance at 21d after dMCAO. **F-G.** Pearson correlation between MBP and SMI-32 staining intensity. **F.** There was a negative correlation between SMI-32 intensity and MBP intensity in aged mice after dMCAO. **G.** There was no significant correlation between SMI-32 intensity and MBP intensity in young mice after dMCAO.

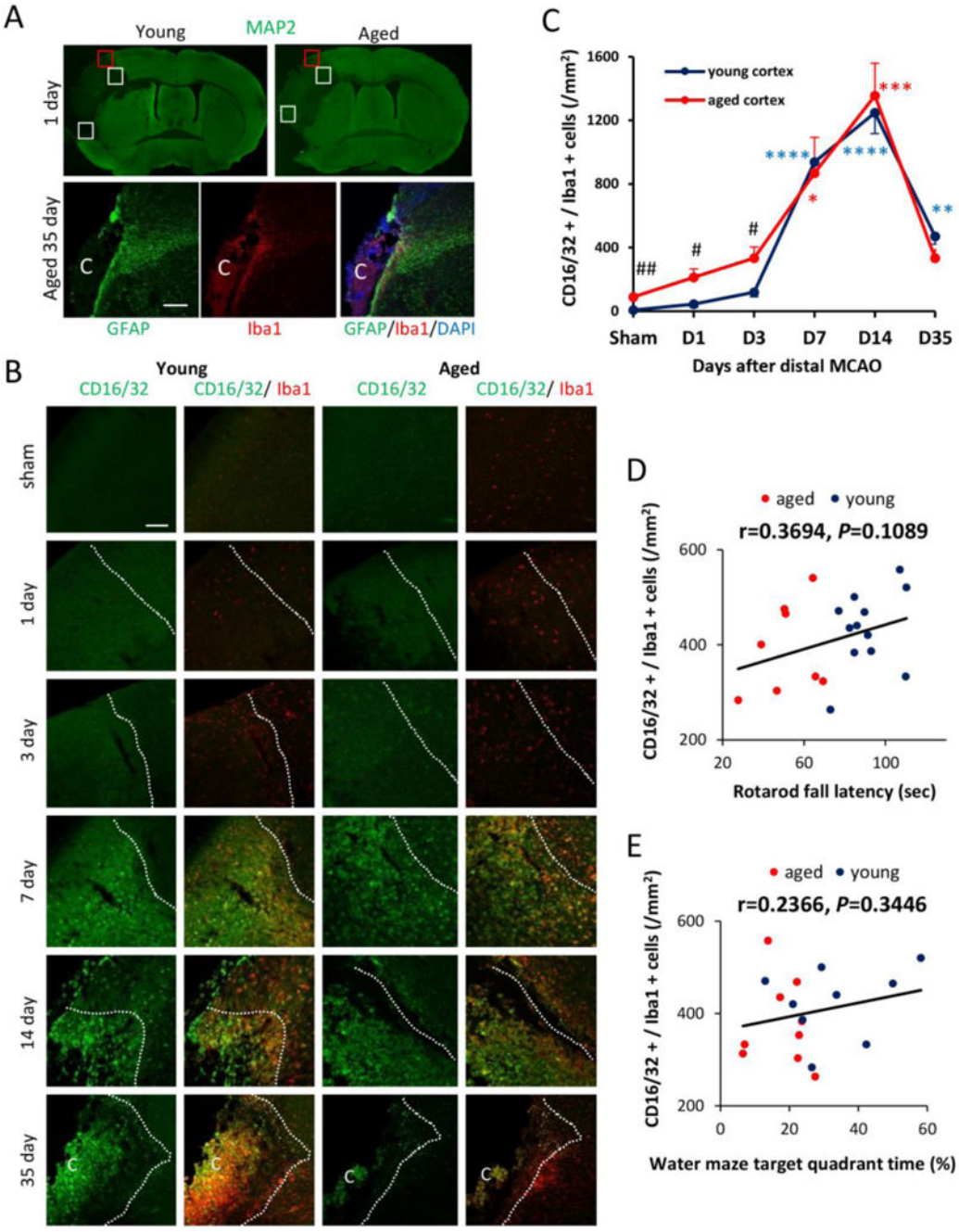

Fig. 5. M1 microglia/macrophage polarization after dMCAO in young and aged mice

A. Image analysis of microglia/macrophage markers in 3 ipsilateral regions (square boxes) at the inner boundary of the infarct. The boundary of the infarct was identified by the loss of MAP2 staining (upper panel) and the boundary of GFAP$^+$ glial scar (lower panel). Scale bar: 40 μm. The letter C represents the ischemic core. **B.** Representative images of CD16/32 (M1 marker; green) and Iba1 (microglia marker; red) double staining at 1, 3, 7, 14, and 35d after dMCAO or in sham-operated animals. Dotted line designates the infarct borderline. Scale bar: 120 μm. **C.** Quantification of the number of CD16/32$^+$Iba1$^+$ cells in the ischemic border

zone in young adult and aged mice. Values are means ± SEM. n=4 per group. * $p \leq 0.05$, ** $p \leq 0.01$, *** $p \leq 0.001$, **** $p \leq 0.0001$ vs corresponding sham. $^{\#}p \leq 0.05$, $^{\#\#}p \leq 0.01$ young vs aged. **D-E.** Lack of correlation between the number of M1 cells and behavioral performance on the Rotarod at 35d after dMCAO or the Morris water maze memory test at 21d after dMCAO.

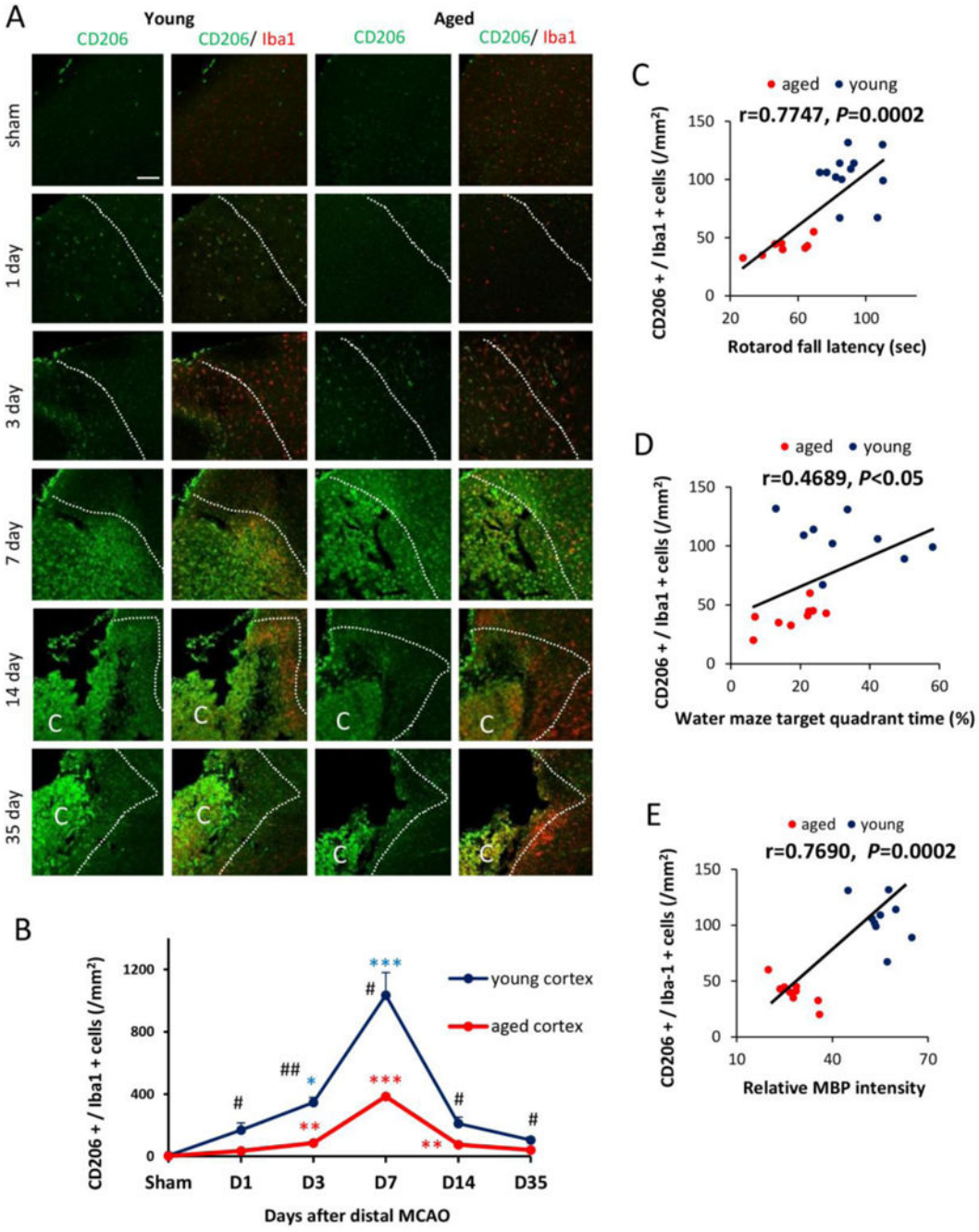

Fig. 6. M2 microglia/macrophage polarization after dMCAO in young and aged mice

A. Representative images of CD206 (M2 marker; green) and Iba1 (red) double staining at 1, 3, 7, 14, and 35d after dMCAO or in sham-operated animals. Dotted line designates the infarct borderline. Scale bar: 120 μm. **B.** Quantification of the number of $CD206^{+}Iba1^{+}$ cells in the ischemic border zone in young adult and aged mice. Values are means ± SEM. n=4 per group. *$p \leq 0.05$, **$p \leq 0.01$, ***$p \leq 0.001$, vs corresponding sham. $^{\#}$ $p \leq 0.05$, $^{\#\#}$ $p \leq 0.01$ young vs aged. **C-D.** Pearson correlation between the number of M2 cells and behavioral performance on the Rotarod or Morris water maze memory tests. **C.** There was a positive

correlation between the number of M2 microglia/macrophage and Rotarod performance at 35d after dMCAO. **D.** There was a positive correlation between the number of M2 microglia/macrophage and water maze performance at 21d after dMCAO. **E.** There was a positive correlation between the number of M2 microglia/macrophage and MBP staining intensity at 35d after dMCAO.